Room-temperature cavity quantum electrodynamics with strongly coupled Dicke states

Room-temperature cavity QED with strongly-coupled Dicke states

Jonathan D. Breeze,[1,2,*] Enrico Salvadori,[3,4,5] Juna Sathian,[1] Neil McN. Alford,[1,2] and Christopher W.M. Kay[3,4]

[1]*Department of Materials, Imperial College London, Exhibition Road, London, SW7 2AZ, UK.*

[2]*London Centre for Nanotechnology, Imperial College London, Exhibition Road, London, SW7 2AZ, UK.*

[3]*Institute of Structural & Molecular Biology, University College London, Gower Street, London, WC1E 8BT, UK.*

[4]*London Centre for Nanotechnology, 17-19 Gordon Street, London, WC1H 0AH, UK.*

[5]*School of Biological and Chemical Sciences, Queen Mary University of London, Mile End Road, London, E1 4NS, UK.*

Collective light-matter interactions are fundamental to cavity quantum electrodynamics (cQED) [1]. A key feature is the *strong coupling regime*, where excitations are coherently transferred between different quantum systems over timescales significantly shorter than their lifetimes. A striking example is the Dicke state [2], where excitations are symmetrically distributed throughout an ensemble of spins or two-level atoms. Dicke states coupled to electromagnetic radiation have been realised experimentally for atomic gases in high-finesse optical cavities [3], emitters near plasmonic nanoparticles [4], electron spins coupled to superconducting qubits [5, 6] and sub-Hertz linewidth super-radiant lasers [7, 8]. Typically in these applications, cryogenic cooling is required to polarize the spin population and mitigate decoherence. Here we report strong coupling and collective Rabi oscillations at room-temperature between an optically excited spin-triplet ensemble within pentacene-doped *p*-terphenyl and a cavity mode supported by a strontium titanate dielectric resonator at 1.45 GHz. The spin ensemble becomes highly correlated through stimulated emission, resulting in cascading entangled Dicke states with suppressed decoherence due to a cavity

* jonathan.breeze@imperial.ac.uk

protection effect [9–11].

The strong coupling regime can be achieved for single quantum emitters interacting with photons within electromagnetic fields through their electric dipole moment [12], however the magnetic coupling strength of single spins to photons is typically far too weak at microwave frequencies. By placing a spin in a resonant cavity, the coupling can be enhanced through the Purcell effect [13] where the local density of photonic states is modified by the geometry. The coupling strength of a single spin to a photon is then given by $g_{\rm s} = \gamma\sqrt{\mu_0\hbar\omega_{\rm c}/2V_{\rm m}}$, where γ is the electron gyromagnetic ratio, μ_0 is the permeability of free-space, $\hbar$ is the reduced Planck constant, $\omega_{\rm c}$ is the angular frequency of the cavity field and $V_{\rm m}$ is the magnetic mode volume. Furthermore, the spin-photon coupling strength $g_{\rm e}$ for an ensemble of N spins is enhanced by a factor $\sqrt{N}$ [6, 14]. Hence, for a sufficient number of spins N and small mode volume $V_{\rm m}$, it should be possible for the ensemble spin-photon coupling strength to exceed both the decay rate of the cavity mode $\kappa_{\rm c}$ and the spin dephasing rate of the spins $\kappa_{\rm s}$, taking the system into the strong coupling regime.

In order to satisfy this condition, we utilise a system comprising spin-triplets in pentacene molecules to generate a polarized (inverted) population of N spins and a cavity with small magnetic mode volume, $V_{\rm m} \sim 10^{-5}\lambda^3$, where λ is the free-space wavelength. Following photo-excitation of pentacene in zero magnetic field, the non-degenerate X, Y, Z sub-levels of the T_1 spin-triplet are rapidly populated in the ratios $0.76 : 0.16 : 0.08$, respectively [15] (see Fig. 1a). The initial inversion is $S^z \approx 0.8\,N$, where N is the number of pentacene molecules excited into either the $|e\rangle \equiv |X\rangle$ or $|g\rangle \equiv |Z\rangle$ states. The state $|Y\rangle$ does not play a significant role and shall not be considered further. At zero magnetic field the $|e\rangle$ and $|g\rangle$ states have a frequency splitting of $\omega_{\rm s}/2\pi \approx 1.45$ GHz. The cavity is similar to the one reported for a miniaturised room-temperature maser which uses a hollow cylinder of strontium titanate (STO), but houses a pentacene-doped p-terphenyl crystal with a much higher concentration of 0.053% mol/mol than in previous studies [16, 17]. The $\mathrm{TE}_{01\delta}$ mode has a frequency tuned to the $\langle e\rangle \leftrightarrow \langle g\rangle$ spin transition, $\omega_{\rm c} \approx \omega_{\rm s} \approx 2\pi \times 1.45$ GHz. This mode has a magnetic field dipole directed along the cylindrical axis (Fig. 1b) which, via the S^y spin-operator, induces transitions between the $|e\rangle \leftrightarrow |g\rangle$ states in suitably aligned pentacene molecules. STO has a high electric permittivity ($\varepsilon_r \approx 320$) that allows a sub-wavelength ($\lambda_0/18 \sim 1$ cm) cavity to be constructed with a mode volume $V_{\rm m}$ of 0.25 cm^3. An optical parametric oscillator (OPO) generated $\lambda \sim 592$ nm pulses of 5.5 ns duration and energy up to 15 mJ at a repetition rate

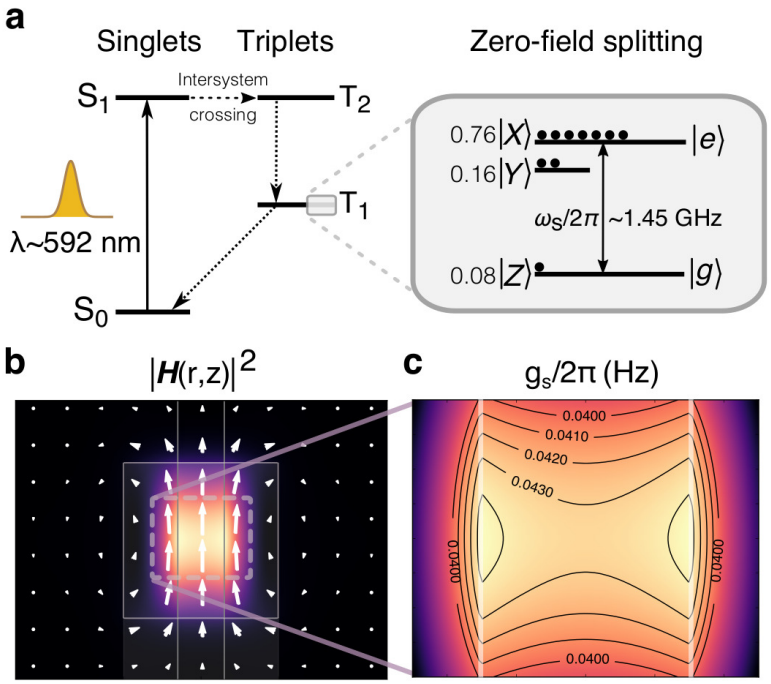

FIG. 1. **Pentacene:*p*-terphenyl/STO cQED system. a**, Simplified Jablonski diagram showing optical pumping scheme that prepares an inverted population. The $|X\rangle \equiv |e\rangle$ and $|Z\rangle \equiv |g\rangle$ triplet sub-levels constitute a two-level system of pseudo spin-1/2 particles with initial relative population 9:1. The difference in energy between the $|e\rangle$ and $|g\rangle$ states is $\hbar\omega_{\rm s}$, where $\omega_{\rm s} \approx 2\pi \times 1.45$ GHz. **b**, Distribution of magnetic energy density within a cross-section of the $\mathrm{TE}_{01\delta}$ mode supported by the cavity. White arrows indicate the magnetic field vector. **c**, Region illuminated by optical pulse. The magnetic field directly maps to the single spin-photon coupling $g_{\rm s}$, for a cylindrical region of diameter 3 mm and height 4 mm, where the pentacene:*p*-terphenyl crystal resides.

of 10 Hz. The 4 mm diameter (Gaussian profile) beam of the OPO was focussed onto the 3 mm diameter pentacene-doped *p*-terphenyl crystal by the high refractive index ($n \sim 2.6$) of the STO. Numerical modelling of the penetration of optical pulses into the pentacene-doped *p*-terphenyl allowed the number N of excited pentacene molecules to be estimated [18] and revealed that the spin-triplet yield is a linear function of the incident optical pulse energy (see Supplementary Information). For an optical pulse energy of 15 mJ, the number of pentacene molecules N excited into the $|e\rangle$ and $|g\rangle$ states was estimated to be $\sim 7 \times 10^{14}$, with an initial inversion $S^z \sim 6 \times 10^{14}$.

The microwave magnetic energy-density (Fig. 1b) can be mapped directly to the single spin-photon coupling in the central region of the cavity housing the pentacene molecules (Fig.

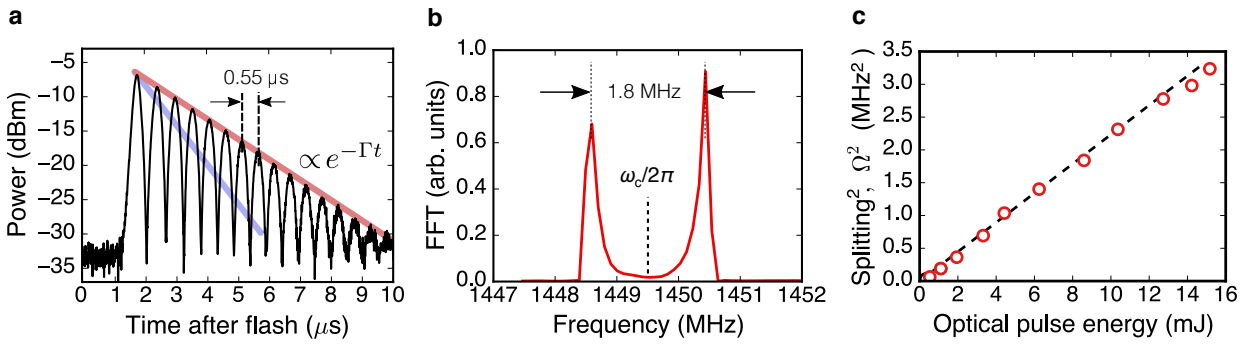

FIG. 2. **Measured microwave emission.** **a**, Rabi oscillations from photo-excited pentacene:*p*-terphenyl spin-ensemble coupled to the STO cavity. The initial burst builds up from thermal photons and follows classical laws since the spin-spin correlation and spin-photon coherence has yet to build up. The peak microwave output power is -6.8 dBm. Subsequent oscillations in the microwave power, with period 0.55 μs and decay rate Γ, are due to the collective exchange of energy between the correlated ensemble Dicke state and the cavity mode. The blue line shows the expected decay of an empty cavity ($\propto e^{-\kappa_c t}$). **b**, Fourier analysis of the signal for a cavity frequency of $\omega_c/2\pi = 1.4495$ GHz and 15 mJ optical pulse energy reveals that ensemble spin-coupling has split the normal modes, yielding a Rabi frequency of $\Omega/2\pi \sim 1.8$ MHz. **c**, Increasing the laser pulse energy excites more pentacene molecules into spin-triplets and therefore increases the ensemble spin-photon coupling (and hence normal-mode Rabi splitting) with a $\sqrt{N}$ dependence. This graph confirms that the square of the splitting is linearly dependent on the optical pump pulse energy and hence N.

1c). Within the region illuminated by the optical pulse, the single spin-photon coupling is $g_s/2\pi = 0.042 \pm 0.002$ Hz. An estimate of the ensemble spin-photon coupling strength is therefore $g_e \approx g_s\sqrt{N} \approx 7\ \mu s^{-1} \approx 2\pi \times 1.1$ MHz. The cavity mode decay rate (linewidth) was measured to be $\kappa_c = 1.1\ \mu s^{-1}$ and the spin decoherence rate of the transition was taken from reported room-temperature free induction decay measurements of the spin dephasing time, $T_2^* = 2.9\ \mu$s [19], yielding a rate of $\kappa_s = 2/T_2^* \approx 0.7\ \mu s^{-1}$. The spin-lattice relaxation rate and decay rates of the triplet sub-levels back to the singlet ground state are at least an order of magnitude slower than the spin dephasing rate so can be neglected [20]. Thus, the system is expected to be within the strong coupling regime since the predicted ensemble spin-photon coupling is an order of magnitude greater than both the cavity decay and spin dephasing rates, $g_e \gg \kappa_c, \kappa_s$, with cooperativity $C = 4g_e^2/\kappa_c\kappa_s \approx 250$.

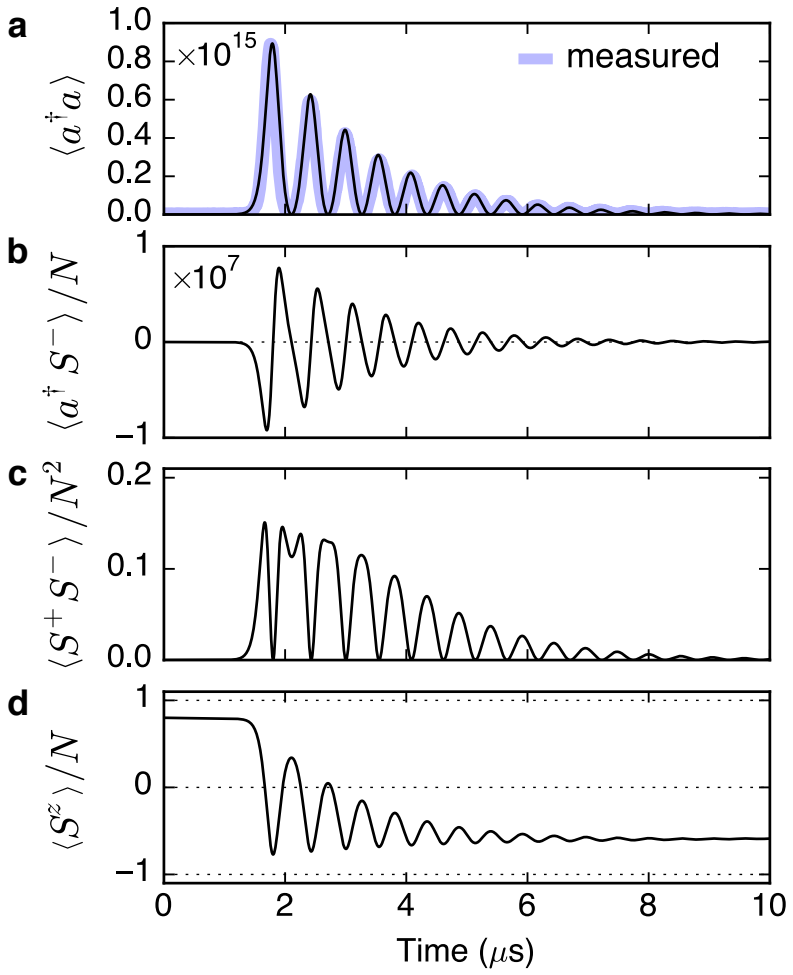

FIG. 3. **Modelled dynamics using master equations.** **a**, The expectation value of the cavity photon number $n = \langle a^\dagger a \rangle$, agrees well with the inferred population from measurement of the microwave power. **b**, Negative values of the spin-photon coherence $\langle a^\dagger S^- \rangle$ correspond to exchange of excitations from the collective spins to the cavity mode and positive values from the cavity mode to the collective spins. **c**, The spin-spin correlation $\langle S^+ S^- \rangle$, a measure of the degree of multipartite entanglement of the spins, is maximal when the inversion is zero. **d**, The inversion S^z, initially at $0.8N$, stays fairly constant until the emergence of the first microwave burst. It subsequently oscillates through the Rabi cycles, coming to rest in a negative yet still spin-polarized state, where the majority of electrons reside in the lower $|g\rangle$ state.

Stimulated emission, due to the population inversion established by the optical pulse, amplifies the thermal cavity photon population ($\bar{n} \sim 4 \times 10^3$), resulting in a buildup of electromagnetic energy in the cavity, *i.e.* masing [21]. The instantaneous microwave power coupled out of the cavity tuned to a frequency of $\omega_c = 2\pi \times 1.4495$ GHz and an optical pulse

of energy 15 mJ is shown in Fig. 2a. There is a short delay of the order of a microsecond until the microwave signal emerges, after which it oscillates with a period of around half a microsecond, whilst decaying at rate Γ over the course of 10 μs. Fourier analysis revealed a normal mode-splitting (Rabi frequency) of $\Omega = 2g_{\mathrm{e}} \approx 11.3\ \mu\mathrm{s}^{-1} \approx 2\pi \times 1.8$ MHz (see Fig. 2b), indicating that the cavity mode and collective spin state have hybridised to form a collective spin-photon polariton and that the strong coupling condition is satisfied, with cooperativity $C \sim 190$. As the optical pump pulse energy was varied from 0 to 15 mJ to excite increasing numbers of pentacene molecules, the normal-mode splitting increased as $\sqrt{N}$ as shown in Fig. 2c, confirming the ensemble spin-photon coupling scaling predicted by the Tavis-Cummings model for a spin-ensemble [22].

For a single excitation at resonance ($\omega_{\mathrm{c}} = \omega_{\mathrm{s}}$), the eigenstates are a coherent superposition of two basis states: the spin-mode and the cavity mode. If $|0\rangle_{\mathrm{c}}$ and $|1\rangle_{\mathrm{c}} = a^{\dagger}|0\rangle_{\mathrm{c}}$ are the possible states of the cavity mode and $|0\rangle_{\mathrm{s}}$ and $|1\rangle_{\mathrm{s}} = a^{\dagger}|0\rangle_{\mathrm{s}}$ are the possible states of the spin-mode, then the two eigenstates are $|+\rangle = \frac{1}{\sqrt{2}}\left(|1\rangle_{\mathrm{s}}|0\rangle_{\mathrm{c}} + |0\rangle_{\mathrm{s}}|1\rangle_{\mathrm{c}}\right)$ and $|-\rangle = \frac{1}{\sqrt{2}}\left(|1\rangle_{\mathrm{s}}|0\rangle_{\mathrm{c}} - |0\rangle_{\mathrm{s}}|1\rangle_{\mathrm{c}}\right)$, separated in energy by $\hbar\Omega = 2\hbar g_{\mathrm{e}}$. In this system, there are many more excitations so to describe the dynamical behaviour of the Dicke system we derived Lindblad master equations for the reduced spin-photon density matrix within the Born-Markov approximation [7, 23]. Here we used the Tavis-Cummings Hamiltonian and a Liouvillian that accounted for decoherence due to cavity decay, spin dephasing and spin-lattice relaxation. A system of coupled differential equations was derived for the expectation values of relevant variables using a cumulant expansion truncated to third-order [24] (see Supplementary Information). The dynamical behaviour of the expectation values of the cavity photon population, spin-photon coherence, spin-spin correlation and inversion are shown in Fig. 3, where the photon population $\bar{n} = \langle a^{\dagger}a \rangle$ is in excellent agreement with that inferred from the measured microwave power. The delay between photo-excitation and the emergence of the first microwave burst can be explained in terms of the spin-spin correlation $\langle S^{+}S^{-} \rangle$. Initially, the spins are not correlated but through stimulated emission of photons into the cavity become increasingly correlated, leading to the buildup of a macroscopic collective dipole. The maximum expectation value of the modelled spin-spin correlation, $\langle S^{+}S^{-} \rangle / N^2 \approx 0.15$ is not much less than the theoretical maximum of 0.25 (see Supplementary Information). The discrepancy being mostly due to the imperfect initialisation of the spin population polarization. The collective spin-spin correlation $\langle S^{+}S^{-} \rangle$ reveals the degree

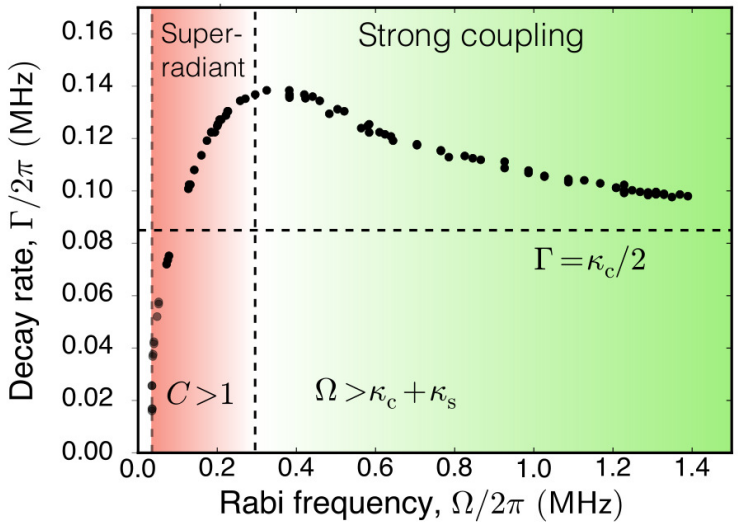

FIG. 4. **Cavity protection due to inhomogeneous broadening.** The vertical dashed lines marks the onset of super-radiant masing (where the cooperativity $C > 1$) and the strong coupling regime where $\Omega = 2g_e > \kappa_c + \kappa_s$, the Rabi frequency exceeds the sum of cavity decay and spin decoherence rates. As the Rabi frequency increases, Γ, the decay rate of the collective spin-photon polariton decreases, asymptotically approaching half the cavity decay rate $\kappa_c/2$ (horizontal dashed line).

of transient multipartite entanglement within the symmetric Dicke states, the entanglement resulting from the ambiguity in being able to assign emission or absorption of photons to specific molecules [1]. For the $N = 2$ case, the maximally entangled $(|e, g\rangle + |g, e\rangle)/\sqrt{2}$ state is a Bell state. Once the collective dipole emerges there is coherent oscillatory exchange of excitations with the cavity mode at the Rabi frequency Ω, persisting for up to 10 μs.

The collective spin-photon polariton decay rate Γ as a function of Rabi frequency (for optical pump pulses in the 0 to 10 mJ range) is shown in Fig. 4. Above maser threshold where the cooperativity $C > 1$ and below the strong coupling regime threshold, the system is super-radiant and the rate of emission is proportional to N^2. The decay rate Γ increases until the Rabi frequency is equal to the sum of the cavity decay and spin decoherence rates, $\Omega = 2g_e \sim \kappa_c + \kappa_s$ and the decay rate $\Gamma \sim (\kappa_c + \kappa_s)/2$. As the Rabi frequency (and ensemble spin-photon coupling) increases and the system goes further into the strong-coupling regime, the ensemble spin-photon polariton decay rate Γ begins decreasing asymptotically towards half the cavity decay rate, $\kappa_c/2$, implying that the spin dephasing rate is suppressed. This so-called *cavity protection* effect, associated with non-Markovian memory effects, is attributed

to inhomogeneous broadening of spin transitions with non-Lorentzian lineshapes [9–11].

To conclude, this system, which was recently used to demonstrate a solid-state room-temperature maser [16, 17, 21], also shows promise as a platform for exploring cavity quantum electrodynamics, spin memories for quantum information processing [14] and quantum-enhanced technologies such as metrology, sensing and communications.

ACKNOWLEDGEMENTS

The authors thank Ke-Jie Tan for supplying the pentacene:*p*-terphenyl crystal, Andrew Horsfield, Stuart Bogatko, Riccardo Montis, Benjamin Richards, Mark Oxborrow and Myungshik Kim for helpful discussions. This work was supported by the UK Engineering and Physical Sciences Research Council through grants EP/K011987/1 (IC) and EP/K011804/1 (UCL).

AUTHOR CONTRIBUTIONS

Experiments were performed by J.D.B., E.S., J.S. and C.W.M.K. Data was processed by J.D.B. and C.W.M.K. Theory was developed by J.D.B. who also performed simulations of quantum master equations, optical pulse penetration and cavity design. The paper was written by J.D.B. with assistance by C.W.M.K. and additional editing by E.S. and N.McN.A. The study was conceived by J.D.B. E.S., N.McN.A. and C.W.M.K.

AUTHOR INFORMATION

The authors declare no competing financial interests. Readers are welcome to comment on the online version of this article at www.nature.com/nature. Correspondence and requests for materials should be addressed to J.D.B. (jonathan.breeze@imperial.ac.uk).

METHODS

Experimental setup. The cavity was constructed from a hollow cylindrical single-crystal of strontium titanate (STO) containing a 0.053% pentacene-doped *p*-terphenyl crystal (diameter 3 mm, height 8 mm). The STO cylinder was placed upon a cylindrical sapphire

disc and housed within a cylindrical copper enclosure. The cavity was directly coupled to a digital storage oscilloscope (Keysight MSOX6004A, 20 GSa/s sampling-rate, 6 GHz bandwidth) using a small loop antenna with coupling coefficient, $k = 0.2$. An additional weakly coupled (-35 dB) antenna, directional coupler (-20 dB) and amplifier (40 dB) allowed transmission measurements of the cavity to made using a vector network analyzer (Agilent 8520E), revealing the resonant frequency and loaded quality-factor (Q) of the $TE_{01\delta}$ mode to be $\omega_c \sim 2\pi \times 1.45$ GHz and 8,500 respectively. A Nd:YAG pumped optical parametric oscillator (OPO, Continuum Surelite Plus SL I-20) generated 592 nm wavelength optical pulses of 5.5 ns duration and energy up to 15 mJ at a repetition rate of 10 Hz. The optical pump pulse energies were measured using a beam splitter and an optical energy meter (Gentec-EO Maestro).

Crystal growth. The pentacene:*p*-terphenyl crystal was grown as per the previously reported method [16, 17] but with higher concentration of pentacene (see Supplementary Information for details).

Cavity photon number from microwave power. The expectation value of the photon number as a function of time was extracted from the measured microwave power $P(t)$ using the expression $\bar{n}(t) = \langle a^\dagger a \rangle = P(t)(1+k)/\hbar\omega_c\kappa_c k$, where k is the coupling coefficient ($k = 0.2$), $\hbar$ is the reduced Planck constant and ω_c and κ_c the cavity frequency and decay rate respectively.

REFERENCES

[1] Haroche, S. & Raimond, J.-M. *Exploring the quantum: Atoms, cavities, and photons* (Oxford university press, 2006).

[2] Dicke, R. H. Coherence in spontaneous radiation processes. *Phys. Rev.* **93**, 99 (1954).

[3] Baumann, K., Guerlin, C., Brennecke, F. & Esslinger, T. Dicke quantum phase transition with a superfluid gas in an optical cavity. *Nature* **464**, 1301–1306 (2010).

[4] Pustovit, V. N. & Shahbazyan, T. V. Cooperative emission of light by an ensemble of dipoles near a metal nanoparticle: The plasmonic Dicke effect. *Phys. Rev. Lett.* **102**, 077401 (2009).

[5] Zhu, X. *et al.* Coherent coupling of a superconducting flux qubit to an electron spin ensemble in diamond. *Nature* **478**, 221–224 (2011).

[6] Sandner, K. *et al.* Strong magnetic coupling of an inhomogeneous nitrogen-vacancy ensemble

to a cavity. *Phys. Rev. A* **85**, 053806 (2012).

[7] Meiser, D., Ye, J., Carlson, D. & Holland, M. Prospects for a millihertz-linewidth laser. *Phys. Rev. Lett.* **102**, 163601 (2009).

[8] Bohnet, J. G. *et al.* A steady-state superradiant laser with less than one intracavity photon. *Nature* **484**, 78–81 (2012).

[9] Diniz, I. *et al.* Strongly coupling a cavity to inhomogeneous ensembles of emitters: Potential for long-lived solid-state quantum memories. *Phys. Rev. A* **84**, 063810 (2011).

[10] Krimer, D. O., Putz, S., Majer, J. & Rotter, S. Non-markovian dynamics of a single-mode cavity strongly coupled to an inhomogeneously broadened spin ensemble. *Phys. Rev. A* **90**, 043852 (2014).

[11] Putz, S. *et al.* Protecting a spin ensemble against decoherence in the strong-coupling regime of cavity QED. *Nat. Phys.* **10**, 720–724 (2014).

[12] Yoshie, T. *et al.* Vacuum rabi splitting with a single quantum dot in a photonic crystal nanocavity. *Nature* **432**, 200–203 (2004).

[13] Purcell, E. Spontaneous emission probabilities at radio frequencies. *Phys. Rev.* **69**, 681 (1946).

[14] Amsüss, R. *et al.* Cavity QED with magnetically coupled collective spin states. *Phys. Rev. Lett.* **107**, 060502 (2011).

[15] Sloop, D. J., Yu, H., Lin, T. & Weissman, S. I. Electron spin echoes of a photoexcited triplet: Pentacene in p-terphenyl crystals. *J. Chem. Phys.* **75**, 3746 (1981).

[16] Breeze, J. *et al.* Enhanced magnetic Purcell effect in room-temperature masers. *Nat. Comms.* **6** (2015).

[17] Salvadori, E. *et al.* Nanosecond time-resolved characterization of a pentacene-based room-temperature maser. *Sci. Rep.* **7**, 41836 (2017).

[18] Takeda, K., Takegoshi, K. & Terao, T. Zero-field electron spin resonance and theoretical studies of light penetration into single crystal and polycrystalline material doped with molecules photoexcitable to the triplet state via intersystem crossing. *J. Chem. Phys.* **117**, 4940–4946 (2002).

[19] Yang, T.-C., Sloop, D., Weissman, S. & Lin, T.-S. Zero-field magnetic resonance of the photo-excited triplet state of pentacene at room temperature. *J. Chem. Phys.* **113**, 11194–11201 (2000).

[20] Yu, H.-L., Lin, T.-S., Weissman, S. & Sloop, D. J. Time resolved studies of pentacene triplets

by electron spin echo spectroscopy. *J. Chem. Phys.* **80**, 102–107 (1984).

[21] Oxborrow, M., Breeze, J. & Alford, N. Room-temperature solid-state maser. *Nature* **488**, 353–356 (2012).

[22] Tavis, M. & Cummings, F. W. Exact solution for an N-molecule radiation-field Hamiltonian. *Phys. Rev.* **170**, 379 (1968).

[23] Carmichael, H. J. *Statistical Methods in Quantum Optics 1: Master Equations and Fokker-Planck Equations* (Springer, 2003).

[24] Kubo, R. Generalized cumulant expansion method. *J. Phys. Soc. Jap.* **17**, 1100–1120 (1962).